ICAS 2016
30th Congress of the International Council of the Aeronautical Sciences
DCC, Daejeon, Korea ; September 25-30, 2016

ELASTIC MODES ADAPTIVE CANCELLATION ALGORITHM FOR THE A330 MRTT FLYING BOOM CONTROL LAWS

Rodney Rodríguez Robles, Alberto Sanz de Blas
Airbus Defence and Space, Getafe, Spain
rodney.rodriguez@airbus.com, alberto.sanz@airbus.com

Keywords: *Aeroservoelastic Coupling, Flying Boom, Extended Adaptive Spatial Filtering*

Abstract

The present paper describes a novel adaptive algorithm developed to cancel the elastic modes component in the feedback of the Flying Boom Control Laws maintaining unaltered the sensed rigid system dynamics. In contrast to other existing techniques, the Elastic Modes Adaptive Cancellation (EMAC) algorithm uses minimum information of the system and only requires two sensors to cancel all the elastic modes of the structure present in the feedback signals. The online modal identification technique implemented in the EMAC, adaptively reconfigure an internal signals fusion algorithm, providing an excellent elastic component suppression performance for elastic systems with fast time-varying geometries and exogenous boundary conditions with discrete changes.
Robustness and performance analyses of the proposed algorithm have been carried out with simulation results from different test benches, including results from flight test campaigns with the A330 MRTT and the A310MRTT.
The paper is structured so as to describe the entire design process of the algorithm, from the initial definition of the high level requirements to the final implementation and validation.

1 Nomenclature and abbreviations

f = Nonlinear system dynamics function
g = System observation function
x = State variables that describe the dynamic evolution of the rigid system
η = Generalized elastic displacements
u = Control inputs
w = External disturbances
y = Output measurement
r = Rigid dynamics output measurement
v = Measurement errors
β = Virtual measured signal
ε = Estimation error
t = Time
Δt = Sample time
$\mathbb{R}$ = The set of real numbers
$\mathbb{N}^+$ = The set of positive natural numbers
p = Dimension of state variables vector
N = Dimension of generalized elastic displacement vector
l = Dimension of control inputs vector
L = Telescopic beam length
P = Dimension of external disturbances vector
Q = Dimension of measurement errors vector
S = Number of sensors in a spatial array
m = Dimension of measurement output
n = Discrete-time sample index
F = Flight Control Laws function
F = Measured nozzle forces
H = Filter function
Y = Filtered measurement output
K = Elastic mode shape cancelation parameter
E = Error function
φ = Elastic mode shape
ϕ = Bandwidth power ratio
θ = Spatial filter parameter vector
$\boldsymbol{\Xi}$ = Elastic mode shape matrix
$\boldsymbol{\Phi}$ = Spatial filter matrix
EMAC = Elastic Modes Adaptive Cancellation
ALAS = Automatic Loads Alleviation System
MRTT = Multi Role Tanker Transport

2 Introduction

Along the aerospace history, many are the incidents that have emphasized the important role that aeroservoelastic coupling plays in the stability of controlled vehicles [1, 2]. Instability and handling qualities degradation shall be avoided by supressing the structural elastic modes in the feedback paths of the Control Laws (CLAWS). In the particular case of controlled systems with a very flexible structure, notch filters are no longer a suitable filtering technique to remove the elastic modes from the feedback signals, and it is essential to use alternative methods that minimize the impact on the rigid dynamics component to achieve the required handling qualities level and stability margins. This is the case of the flying boom installed in the A330 MRTT, a flexible slender structure with highly non-linear aerodynamics and elastic characteristics that strongly vary with the flight condition, the operational phase and with the telescopic beam length. The first bending mode frequency of the flying boom in both free-air and coupled conditions (during refuelling operations) lie in the bandwidth of the rigid control frequencies. To suppress this mode without introducing unacceptable phase-loss and attenuation in the sensed rigid dynamics, Airbus Defence and Space developed and patented a spatial filter to mix the attitude and angular rate measured by two different sensors [3].

Figure 1: Refuelling operation with the flying boom system with an A330 MRTT (tanker) and an F-35A Joint Strike Fighter (receiver)

This spatial filter can cancel the first bending structural mode in free air based on the knowledge of the mode shape as a function of the flight condition and the telescopic beam extension. This model based methodology requires an offline fine tuning based on data gathered during an extensive flight test campaign. Moreover, this method lacks of robustness against uncertainties in the modelled plant. To enhance the performance and robustness of the current spatial filter, and to reduce the development time and cost associated to the standard model based design, the Elastic Modes Adaptive Cancellation algorithm was developed. This innovative algorithm is an evolution of the original patent, and has been developed to cancel all existing elastic modes in the feedback path by means of a robust adaptive strategy. The EMAC algorithm identifies the elastic natural frequencies in real time and adaptively adjusts the frequency mixing matrix applied to the measured feedback signals to generate a filtered signal containing only the rigid dynamics of the flying boom, with zero phase-loss and attenuation. Furthermore, the EMAC algorithm could enable the control of the elastic dynamics of the flying boom using a dedicated control law in combination with the CLAWS for the rigid dynamics without impacting on the stability margins of the rigid motion.

3 Aeroservoelastic Coupling Suppression

Aeroservolastic coupling suppression is a multidisciplinary technology dealing with the interaction of air vehicle non-stationary aerodynamic forces, the structure dynamics and the flight control system dynamics. Several studies have been conducted assessing strategies and methodologies in the design of active flight control algorithms to favourably modify the aeroelastic dynamics of the system, or to simply decouple the rigid and elastic measured dynamics to minimize the adverse effects on the stability margins and handling qualities. In this section we will address the decoupling problem and expose different solutions that have been evaluated during the development of the EMAC algorithm.

Without loss of generality, the aeroservoelastic dynamics of a time-varying system can be described as

$$\begin{bmatrix}\dot{\boldsymbol{x}}\\ \dot{\boldsymbol{\eta}}\end{bmatrix} = \boldsymbol{f}(\boldsymbol{x},\boldsymbol{\eta},\boldsymbol{u},\boldsymbol{w},t) \tag{1}$$

$$\boldsymbol{y} = \boldsymbol{g}(\boldsymbol{x},\boldsymbol{\eta},\boldsymbol{u},\boldsymbol{v},t) \tag{2}$$

where $\boldsymbol{x} \in \mathbb{R}^p$ is a collection of state variables that describe the dynamic evolution of the rigid system, $\boldsymbol{\eta} \in \mathbb{R}^N$ is the vector of generalized elastic displacements, $\boldsymbol{u} \in \mathbb{R}^l$ is the control input, $\boldsymbol{w} \in \mathbb{R}^P$ contains the external disturbances, $\boldsymbol{v} \in \mathbb{R}^Q$ is the vector of measurement errors, $\boldsymbol{y} \in \mathbb{R}^m$ is the output measurement and t is the time, denoting that both the system nonlinear dynamics defined by $\boldsymbol{f}: \mathbb{R}^{p+N+l+P+1} \to \mathbb{R}^{p+N}$ and the system observation characteristics defined by $\boldsymbol{g}: \mathbb{R}^{p+N+l+Q+1} \to \mathbb{R}^m$, are time varying functions that depends on exogenous boundary conditions. Aeroservoelastic coupling phenomenon is originated when the CLAWS feedback contains not only the rigid state variables but also the generalized elastic displacements.

$$\boldsymbol{u} = \boldsymbol{F}(\boldsymbol{y},t) = \boldsymbol{F}(\boldsymbol{x},\boldsymbol{\eta},\boldsymbol{u}(t-\Delta t),\boldsymbol{v},t) \tag{3}$$

In this case, if no filtering is applied to the feedback $\boldsymbol{y}$, depending on the flight controls characteristics and on the rigid system modes, the control inputs $\boldsymbol{u}$ could amplify the elastic displacements leading to instability. The objective pursued with the filtering is to eliminate the dependency of the control inputs with the generalized elastic displacements in such a way the CLAWS in (3) could be expressed ideally as

$$\boldsymbol{Y}(\boldsymbol{x},\boldsymbol{u},\boldsymbol{v},t) = \boldsymbol{H}(\boldsymbol{y}(\boldsymbol{x},\boldsymbol{\eta},\boldsymbol{u},\boldsymbol{v},t),t) \tag{4}$$

$$\boldsymbol{u} = \boldsymbol{F}(\boldsymbol{Y},t) \tag{5}$$

with $\boldsymbol{Y} \in \mathbb{R}^m$ is the filtered output measurement and $\boldsymbol{H}$ is the filter function. The selection of the filtering method will condition the closed loop system stability, so it is desirable to design this filter with a trade-off between the attenuation of the elastic modes component and the impact on the rigid state components in the feedback. One of the filtering methods that have been widely used in the aerospace industry to cancel the aeroservoelastic coupling is the use of cascades of notch filters [4]. This approach is suitable for systems with elastic modes frequencies that lie outside the control frequency bandwidth of the augmented system. In other cases, when the system has a very flexible structure, the delay and attenuation introduced by the notch filters in the low-frequency region of the system frequency response make the harmonization between robustness and handling qualities to be hardly achievable during the CLAWS design. Alternative solutions for very flexible systems have been developed to meet the design requirements. In [5] an extended Kalman filter is proposed to attenuate the feedback elastic component at the resonant frequencies using the theoretic model of the rigid system and in [6] a modal filter is used. In addition to these solutions, spatial filtering technique [7] has proved to be a very effective technology that uses a distributed sensors array to cancel the elastic modes components in the feedback signal, assuming the elastic modes shapes are known beforehand (model based). Nevertheless, the number of sensors used is in general greater than twice the number of elastic modes to be suppressed [7].

These alternative solutions, like all model based filtering methods, conventionally lack of robustness and adaptation capabilities against plant uncertainties, cannot cope with fast changes in the structure morphology, and their performance is very sensitive to variations in the exogenous boundary conditions. All these drawbacks have motivated the development of the EMAC algorithm so as to achieve a robust online cancellation of the elastic modes in the feedback using a non-model-based approach.

4 Proposed Algorithm

The Elastic Modes Adaptive Cancellation algorithm uses the output of two measurement sources to generate an extended multi-modal spatial filter. First, a collection of estimation kernels identifies the elastic modes characteristics. Outputs of these kernels are feedforwarded to an algebraic solver, where a

set of virtual signals which are linearly independent with respect to their elastic modes contents is generated. This solver is the responsible of handling the fusion of the virtual signals set to make the user-selected elastic modes unobservable, while maintaining unaltered the sensed rigid dynamics of the nonlinear time-varying system. In parallel, a special observer estimates the exogenous boundary condition acting on the system and accordingly configures the constraints applicable to the distributed constrained estimation kernels. This additional observer is intended to make the filtering robust against undetected exogenous boundary conditions transitions.

4.1 Elastic Modes Estimation Kernels

Each kernel is intended to provide an estimate of the elastic modes displacement, and an estimate of the K_n^i parameters required to cancel a specific elastic mode given two scalar signals y_A and y_B, measured by sensor A and sensor B respectively. These discrete-time scalar signals can be expressed in terms of the sensed rigid and elastic system dynamics as

$$y_n^A = r_n + \sum_{j=1}^{N} \varphi_n^j(\boldsymbol{l}_A)\eta_n^j + v_n^A \tag{6}$$

$$y_n^B = r_n + \sum_{j=1}^{N} \varphi_n^j(\boldsymbol{l}_B)\eta_n^j + v_n^B \tag{7}$$

where $\boldsymbol{l}_A \in \mathbb{R}^3$ and $\boldsymbol{l}_B \in \mathbb{R}^3$ denote the spatial location of sensors A and B respectively. The perfect cancellation parameter for the ith elastic mode K_n^i can be computed imposing that the linear combination of the two measured signals results in the suppression of the $\varphi_n^i(\boldsymbol{l}_A)\eta_n^i$ term in (6), while maintaining unaltered the sensed rigid dynamics denoted by r_n

$$\begin{aligned} K_n^i y_n^A + (1-K_n^i) y_n^B &= r_n \\ &+ \sum_{j=1\neq i}^{N} \left[K_n^i \varphi_n^j(\boldsymbol{l}_A)\eta_n^j \right. \\ &+ \left.(1-K_n^i)\varphi_n^j(\boldsymbol{l}_B)\eta_n^j\right] \\ &+ K_n^i v_n^A + (1-K_n^i) v_n^B \end{aligned} \tag{8}$$

Solving (8) for $K_i(n)$ yields

$$K_n^i = \frac{\varphi_n^i(\boldsymbol{l}_B)}{\varphi_n^i(\boldsymbol{l}_B) - \varphi_n^i(\boldsymbol{l}_A)} \tag{9}$$

In a model based approach, one could use the elastic model to compute the unitary displacements $\varphi_n^i(\boldsymbol{l}_A)$ and $\varphi_n^i(\boldsymbol{l}_B)$ to obtain the theoretic value of the perfect cancellation parameters. However, elastic model uncertainties generally are associated with a degradation of the elastic mode cancellation performance. To prevent this, an online estimator for the K_n^i parameter is used, under the assumption that for both measured signals y_A and y_B, the system rigid dynamics power spectral density is negligible with respect the elastic dynamics power spectral density in a narrow frequency bandwidth Δω centred at the ith elastic mode damped natural frequency ω_i. This is:

$$\phi_A = \frac{\int_{\omega_i-\Delta\omega/2}^{\omega_i+\Delta\omega/2} \sum_{n=-\infty}^{\infty} r_n e^{-j\omega n}\, d\omega}{\int_{\omega_i-\Delta\omega/2}^{\omega_i+\Delta\omega/2} \sum_{n=-\infty}^{\infty} \varphi_n^i(\boldsymbol{l}_A)\eta_n^i e^{-j\omega n}\, d\omega} \ll 1 \tag{10}$$

$$\phi_B = \frac{\int_{\omega_i-\Delta\omega/2}^{\omega_i+\Delta\omega/2} \sum_{n=-\infty}^{\infty} r_n e^{-j\omega n}\, d\omega}{\int_{\omega_i-\Delta\omega/2}^{\omega_i+\Delta\omega/2} \sum_{n=-\infty}^{\infty} \varphi_n^i(\boldsymbol{l}_B)\eta_n^i e^{-j\omega n}\, d\omega} \ll 1 \tag{11}$$

Using (10) and (11), one can ensure that the solution of the following least mean square problem is a quasi-unbiased estimator of the K_n^i parameter

$$\min_{\widehat{K}_n^i} E_n^i = \min_{\widehat{K}_n^i} \sum_{j=1}^{N_i} \left(\widehat{K}_n^i Y_j^A + \left(1-\widehat{K}_n^i\right) Y_j^B\right)^2 \tag{12}$$

$$\begin{aligned} Y_n^J &= H_c(z;\omega_i,\omega_{i-1},\omega_{i+1}) y^J(z) \\ J &= A, B \end{aligned} \tag{13}$$

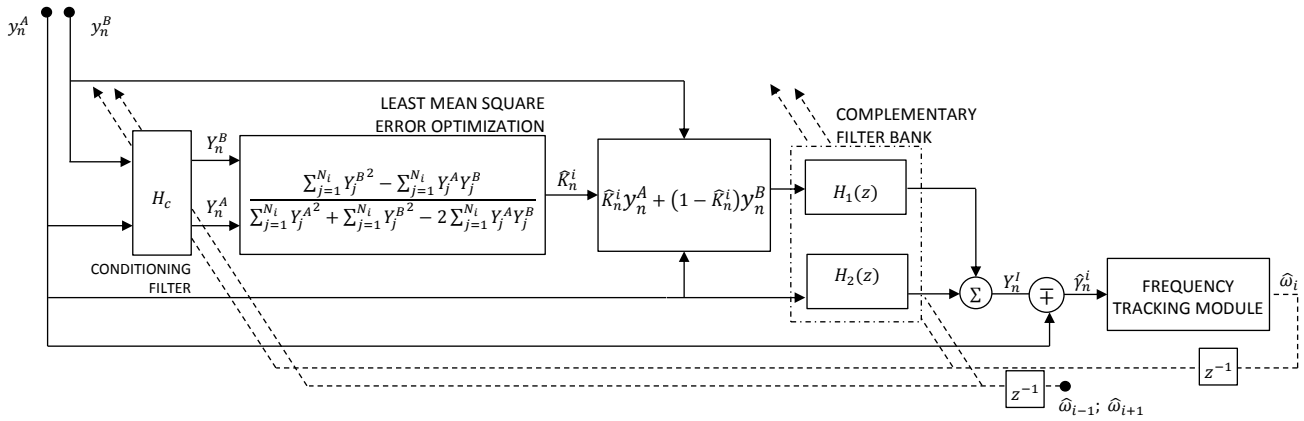

Figure 2: Block diagram of an elastic mode estimation kernel

$N_i \in \mathbb{N}^+$ in (12) is selected to be an integer multiple of $2\pi/\omega_i \Delta t$ to compute the cost function during at least one period of the ith elastic mode. Y_n^A is the output of a parametric digital filter H_c, with y_A and y_B as input signals. This digital filter is composed by a narrow band-pass filter with bandwidth $\Delta\omega_{BP}$ centred at ω_i, combined with two narrow stop-band filters with bandwidth $\Delta\omega_{SB}$ centred at ω_{i-1} and ω_{i+1} respectively. It is intended to isolate the ith elastic mode and avoid possible estimation errors in $\widehat{K}_n^i$ induced by inter-modal interferences. Once Y_j^A and Y_j^B have been calculated, the estimated cancellation parameter $\widehat{K}_n^i$ is computed like

$$\widehat{K}_n^i = \frac{\sum_{j=1}^{N_i} {Y_j^B}^2 - \sum_{j=1}^{N_i} Y_j^A Y_j^B}{\sum_{j=1}^{N_i} {Y_j^A}^2 + \sum_{j=1}^{N_i} {Y_j^B}^2 - 2\sum_{j=1}^{N_i} Y_j^A Y_j^B} \quad (14)$$

Expanding (14), one can demonstrate that the estimation bias in $\widehat{K}_n^i$ is a function of ϕ_A, ϕ_B and the measurements noise.

$$\widehat{K}_n^i = K_n^i + \varepsilon(\phi_A, \phi_B, v_n^A, v_n^B) \quad (15)$$

When (10) and (11) are satisfied, the estimation bias mainly depends on the measurement noise, and so, solution (14) is said to be a quasi-unbiased estimator. This can be achieved by selecting $\Delta\omega_{BP}$ to be small. If (10) and (11) are not satisfied due to the low excitation of the elastic modes, equation (14) for $\widehat{K}_n^i$ is no longer updated and the last value $\widehat{K}_{n-1}^i$is used instead. It has to be noted that so far, all damped natural frequencies of the elastic modes ω_i have been assumed to be known. To complete the non-model based adaptive approach, it is mandatory to close the identification loop and make the estimation kernel independent and self-contained. With this aim, an adaptive frequency estimation module is used to feedback the $\widehat{K}_n^i$ estimator defined in (14). Given a signal containing multiple elastic modes, there are several algorithms that permit to estimate the frequencies at which its power spectral density is maximized [8, 9]. In this case, a fast Fourier transformation has been used in order to estimate the undamped natural frequency of the ith elastic mode.

The signal $\hat{\gamma}_n^i$ to be analysed by the frequency tracking module represent an estimation of i th elastic mode $\hat{\varphi}_n^i(\boldsymbol{l}_A)\hat{\eta}_n^i$ measured at $\boldsymbol{l}_A$. It is computed by means of an auxiliary variable denoted by Y_n^I

$$\hat{\gamma}_n^i = \hat{\varphi}_n^i(\boldsymbol{l}_A)\hat{\eta}_n^i = y_n^A - Y_n^I = \varphi_n^i(\boldsymbol{l}_A)\eta_n^i + \varepsilon_n^i \quad (16)$$

$$\begin{aligned} Y_n^I = H_1(z;\widehat{\omega}_i,\widehat{\omega}_{i-1},\widehat{\omega}_{i+1})\big[\widehat{K}_n^i y_n^A \\ + \big(1-\widehat{K}_n^i\big)y_n^B\big] \\ + H_2(z;\widehat{\omega}_i,\widehat{\omega}_{i-1},\widehat{\omega}_{i+1})y_n^A \end{aligned} \quad (17)$$

$$\begin{aligned} &H_1(z;\omega_i,\omega_{i-1},\omega_{i+1}) \\ &+H_2(z;\omega_i,\omega_{i-1},\omega_{i+1}) = 1 \end{aligned} \quad (18)$$

Y_n^I is the output of a complementary filter bank defined by (18) which ensures the measured rigid dynamics of y_n^A to stays unaltered. This filter bank is composed by a band-pass filter H_1 and a stop-band filter H_2 centred at $\widehat{\omega}_i$. To break the existing algebraic loops within the estimation kernel, all estimated

frequencies are delayed one step time. In order to increase the robustness of the estimation kernel, parameters $\widehat{K}_n^i$ and the estimated elastic modes undamped frequencies $\widehat{\omega}_i$ are forced to be bounded by extreme values obtained from the most critical tolerance combination of the elastic models of the system. This is $\widehat{K}_n^i \in [K_{min}^i, K_{max}^i]$ and $\widehat{\omega}_i \in [\omega_{min}^i, \omega\,_{max}^i]$. These extreme values depend also on the exogenous boundary conditions. With the described structure (depicted in Figure 2), the estimation kernels are able to compute a quasi-unbiased approximation $\widehat{K}_n^i$ of the perfect cancellation parameters K_n^i for each elastic mode, and an estimate of the mode displacements $\hat{\gamma}_n^i$ at sensor location $\boldsymbol{l}_A$.

4.2 Extended Spatial Filter Algebraic Solver

Spatial filters use the information of a sensor array to generate an output signal in which some or all elastic modes have been suppressed. Displacements measured by a sensor s of a spatial sensor array composed by S sensors can be expressed as

$$y_n^s = r_n + \sum_{j=1}^{N} \varphi_n^j(l_s)\eta_n^j + v_n^s \tag{19}$$

And in a more compact form we obtain

$$\boldsymbol{y}_n = r_n\mathbf{1} + \boldsymbol{\Xi}\boldsymbol{\eta}_n + \boldsymbol{v}_n \tag{20}$$

where now $\boldsymbol{y}_n, \boldsymbol{v}_n \in \mathbb{R}^S$, $\mathbf{1} \in \mathbb{R}^S$ is a column vector of ones, and $\boldsymbol{\Xi} \in \mathbb{R}^S \times \mathbb{R}^N$ is a matrix containing all elastic modes unitary displacement at sensors locations.

$$\boldsymbol{\Xi}_{S\times N} = \begin{bmatrix} \varphi_n^1(l_1) & \dots & \varphi_n^N(l_1) \\ \vdots & \ddots & \vdots \\ \varphi_n^1(l_S) & \dots & \varphi_n^N(l_S) \end{bmatrix} \tag{21}$$

In the standard spatial filtering algorithm, given $\boldsymbol{\Xi}$, the N elastic modes component can be suppressed in the filter output Y_n^{SP} imposing once again that the linear combination of the y_n^j signals result in the total cancellation of all existing elastic modes while keeping the measured rigid dynamics unaltered. This can be achieved only if $S \geq N + 1$.

$$Y_n^{SP} = \sum_{j=1}^{N+1} \theta_n^j y_n^j = r_n + \sum_{j=1}^{N+1} \theta_n^j v_n^j \tag{22}$$

In (22), $\boldsymbol{\theta}_n \in \mathbb{R}^{N+1}$ is a time varying coefficient vector to be determined. This equation can be expressed in compact form using (20) and (21)

$$\boldsymbol{\Phi}\boldsymbol{\theta}_n = \begin{bmatrix} 0 \\ \vdots \\ 0 \\ 1 \end{bmatrix} \tag{23}$$

$$\boldsymbol{\Phi} = \begin{bmatrix} \boldsymbol{\Xi}(1\!:\!N+1, 1\!:\!N)^{\mathbf{T}} \\ \mathbf{1}^{\boldsymbol{T}} \end{bmatrix} = \\ = \begin{bmatrix} \varphi_n^1(l_1) & \dots & \varphi_n^1(l_{N+1}) \\ \vdots & \ddots & \vdots \\ \varphi_n^N(l_1) & \dots & \varphi_n^N(l_{N+1}) \\ 1 & \dots & 1 \end{bmatrix} \tag{24}$$

Finally, solving (23) for θ_n yields

$$\boldsymbol{\theta}_n = \boldsymbol{\Phi}^{-1} \begin{bmatrix} 0 \\ \vdots \\ 0 \\ 1 \end{bmatrix} \tag{25}$$

As it can be observed in (25), the standard spatial filtering method requires the matrix $\boldsymbol{\Phi}$ to be nonsingular in order to cancel the N elastic modes. This matrix depends on the sensor locations, which in the most general case cannot be modified, and on the elastic modes of the system. Then, the feasibility and flexibility of the standard spatial filtering method is reduced in comparison with other adaptive techniques. Additionally, in this case, only y_n^A and y_n^B signals are available, so only one elastic mode could be cancelled [3] using (25). To solve this, an extended spatial filtering method has been implemented in the EMAC algorithm. This method uses the estimates $\widehat{K}_n^i$ and $\hat{\gamma}_n^i$ that have been computed by the N interconnected estimation kernels to generate a set of $N-1$ parametric virtual signals $\hat{\beta}_n^s$ that complements y_n^A and y_n^B. These signals are generated as follows:

$$\hat{\beta}_n^s = y_n^A - \sum_{i=1}^{N} \lambda_n^{i,s}\hat{\gamma}_n^i \tag{26}$$

where $\lambda_n^{i,s}$ are parameters that can be modified within the algebraic solver. Using (26), equation (22) can be reformulated

$$Y_n^{EMAC} = \theta_n^1 y_n^A + \theta_n^2 y_n^B + \sum_{j=3}^{N+1} \theta_n^j \hat{\beta}_n^{j-2} = r_n \quad (27)$$

The new system of equations to be solved now depends on $\lambda_n^{i,s}$ parameters so the algebraic solver can modify the new matrix $\hat{\boldsymbol{\Phi}}$ as required, granting that it is nonsingular. This matrix is an approximation of the spatial filter matrix $\boldsymbol{\Phi}$ defined as:

$$\hat{\boldsymbol{\Phi}} = \begin{bmatrix} \hat{\varphi}_n^1(\boldsymbol{l}_A) & \dots & \hat{\varphi}_n^N(\boldsymbol{l}_A) & 1 \\ \hat{\varphi}_n^1(\boldsymbol{l}_B) & \dots & \hat{\varphi}_n^N(\boldsymbol{l}_B) & 1 \\ (1-\lambda_n^{1,1})\hat{\varphi}_n^1(\boldsymbol{l}_A) & \dots & (1-\lambda_n^{N,1})\hat{\varphi}_n^N(\boldsymbol{l}_A) & 1 \\ \vdots & \ddots & \vdots & \vdots \\ (1-\lambda_n^{1,N-1})\hat{\varphi}_n^1(\boldsymbol{l}_A) & \dots & (1-\lambda_n^{N,N-1})\hat{\varphi}_n^N(\boldsymbol{l}_A) & 1 \end{bmatrix}^T \quad (28)$$

Using equation (9) and (28), one can express $\hat{\boldsymbol{\Phi}}$ as a function of $\lambda_n^{i,s}$ and $\hat{K}_n^i$ dividing each row by the estimated elastic mode shape at location l_A denoted by $\hat{\varphi}_n^i(\boldsymbol{l}_A)$ (if $\hat{\varphi}_n^i(\boldsymbol{l}_A)$ is close to zero, affected rows are divided by $\hat{\varphi}_n^i(\boldsymbol{l}_B)$).

$$\hat{\boldsymbol{\Phi}}_0 = \begin{bmatrix} 1 & \dots & 1 & 1 \\ \frac{1}{\hat{K}_n^i - 1} & \dots & \frac{1}{\hat{K}_n^N - 1} & 1 \\ (1-\lambda_n^{1,1}) & \dots & (1-\lambda_n^{N,1}) & 1 \\ \vdots & \ddots & \vdots & \vdots \\ (1-\lambda_n^{1,N-1}) & \dots & (1-\lambda_n^{N,N-1}) & 1 \end{bmatrix}^T \quad (29)$$

Reformulating equation (25) with (29), the EMAC algorithm output Y_n^{EMAC} finally can be expressed as a function of $\lambda_n^{i,s}$ and the signals calculated in the elastic modes observation kernels.

$$\boldsymbol{\theta}_n = \hat{\boldsymbol{\Phi}}_0^{-1}(\lambda_n^{i,s}, \hat{K}_n^i) \begin{bmatrix} 0 \\ \vdots \\ 0 \\ 1 \end{bmatrix} \quad (30)$$

$$Y_n^{EMAC} = \theta_n^1 y_n^A + \theta_n^2 y_n^B + \\ + \sum_{j=3}^{N+1} \theta_n^j \left(y_n^A - \sum_{i=1}^{N} \lambda_n^{i,s-2} \hat{Y}_n^i \right) \quad (31)$$

A schematic block diagram has been depicted in Figure 3 to show the interconnections between the estimation kernels defined in chapter 4.1 and the extended spatial filter algebraic solver.

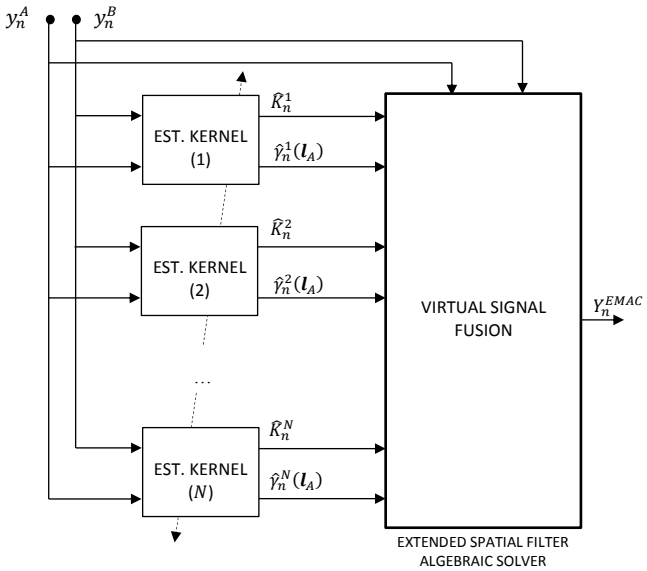

Figure 3: Block diagram showing the estimation kernels interconnections with the extended spatial filter algebraic solver

4.3 Exogenous Boundary Conditions Estimator

Exogenous boundary conditions acting on the system limit the displacements of the structure, and impose certain restrictions in the degrees of freedom of the system that modify its aeroservoelastic properties. Fast discrete changes in the boundary conditions need to be identified in order to reconfigure the filters parameters. To accomplish this, a dedicated observer has been implemented in the EMAC algorithm based on the estimation kernels structure. The basic idea is to monitor the elastic energy in a frequency bandwidth associated to a specific elastic mode, which is characteristic of

a certain boundary condition, and determine whether or not this boundary condition is actually acting on the system. A set of possible boundary conditions is analysed offline and the extreme values K^i_{min}, K^i_{max}, ω^i_{min} and ω^i_{max} are computed using the elastic model of the system. Then, these values are saved in lookup tables within the EMAC algorithm to be used as extreme bounds in each estimation kernel depending on the results of the online estimations of the boundary condition acting on the system.

5 The EMAC Algorithms Applied to the A330 MRTT Flying Boom Control Laws

The flying boom CLAWS of the A330 MRTT is a complex system composed by cascades of multi-loop controllers with multiple feedback signals. CLAWS attitude control signals are the boom pitch angle δ and boom roll angle φ, which have been depicted in Figure 4. In the current flying boom CLAWS version, algorithm [3] is applied to suppress the first longitudinal and lateral bending modes when the CLAWS are in CL2 state, which denotes the flying boom is in free-air condition. The higher frequency elastic modes are attenuated in the feedback paths using a cascade of notch filters.

In CL3 state, which denotes the flying boom is in coupled condition, CLAWS implements the Automatic Loads Alleviation System (ALAS) to minimize the loads measured by sensors located in the nozzle of the telescopic beam. In this coupled operational phase (CL3), a traditional cascade of notch filters is used to attenuate the elastic modes component in the CLAWS feedback signals. It has to be noted that elastic modes shapes φ^i_n and undamped frequencies ω_i of the flying boom suffer great variations during transitions from free air to coupled condition and vice versa due to the discrete changes in the exogenous boundary conditions acting on the structure.

To test the elastic modes suppression performance, the EMAC algorithm has been implemented in an experimental flying boom CLAWS version. For this particular case, an additional conditioning subsystem has been added to the algorithm to generate a suitable signal y^0_n to adaptively suppress the 1st and 2nd elastic modes in free-air, and the 1st elastic mode in coupled condition, with independency of the CLAWS internal state (CL2/CL3). This additional conditioning subsystem fuses the attitude and rate information measured by sensor A and B with the loads F_n measured by

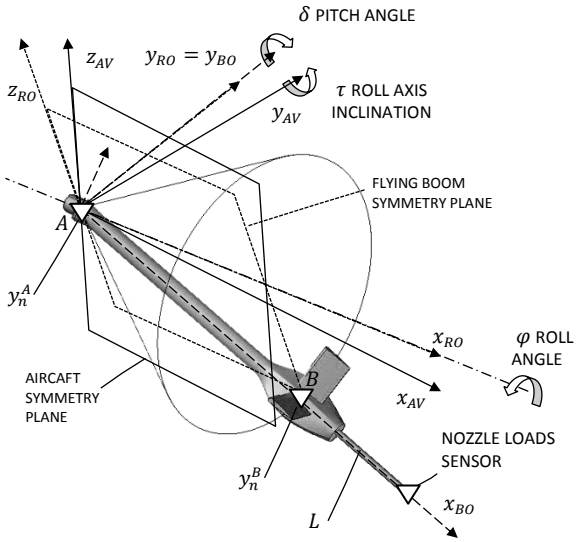

Figure 4: Flying boom reference axis and geometry. Approximated locations of sensors A and B, and the nozzle loads sensor are marked with an inverted triangle

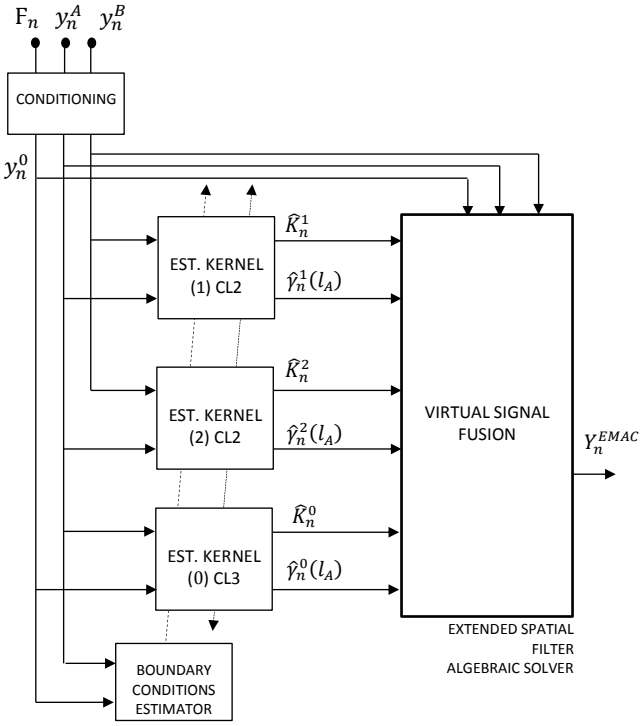

Figure 5: EMAC algorithm for the A330 MRTT flying boom CLAWS

extensometers located at the boom nozzle. A block diagram is depicted in Figure 5 illustrating the configuration of the EMAC algorithm adapted for the flying boom CLAWS feedback signals.

6 Validation Results

With the aim to measure the efficiency and robustness of the EMAC algorithm, an offline test bench has been built. This test bench can be fed with flight test data to obtain the filtered feedback signals with the EMAC algorithm. In a later step, these signals can be compared with the ones generated during the flight test using [3] so as to gauge the efficiency improvement or deterioration achieved using the EMAC algorithm. A total set of 152 flights have been analysed in the test bench, within which buffet exploration tests and hard contact occurrences have been included. Flight test has been carefully selected to cover all possible boom operational conditions and also to cover all possible variations in the elastic properties of the flying boom structure (different telescopic beam length, etc). Recorded data includes flight tests performed with the A330 MRTT and the A310 MRTT.

6.1 Test Bench Results: Buffet Exploration Flight Testing

In this section, offline results obtained using buffet exploration flight testing data are presented. In particular, a flight segment where a severe buffeting phenomenon can be observed has been selected to illustrate the EMAC algorithm performances compared to that of [3]. Data analysed includes a gentle manoeuvre in free-air condition (CL2) at very high speed. During this manoeuvre, the flying boom performs a gradual extension of the telescopic beam up to its maximum value (critical for buffet).

Results depicted in Figure 6 prove that the EMAC algorithm is capable of perfectly cancelling the 1st and 2nd elastic modes in the roll feedback signal as intended. Results for $\widehat{K}_n^1$ parameter indicate that for these particular conditions, sensor *A* is located in a node of the 1st lateral elastic mode as the $\widehat{K}_n^1$ value is very small.

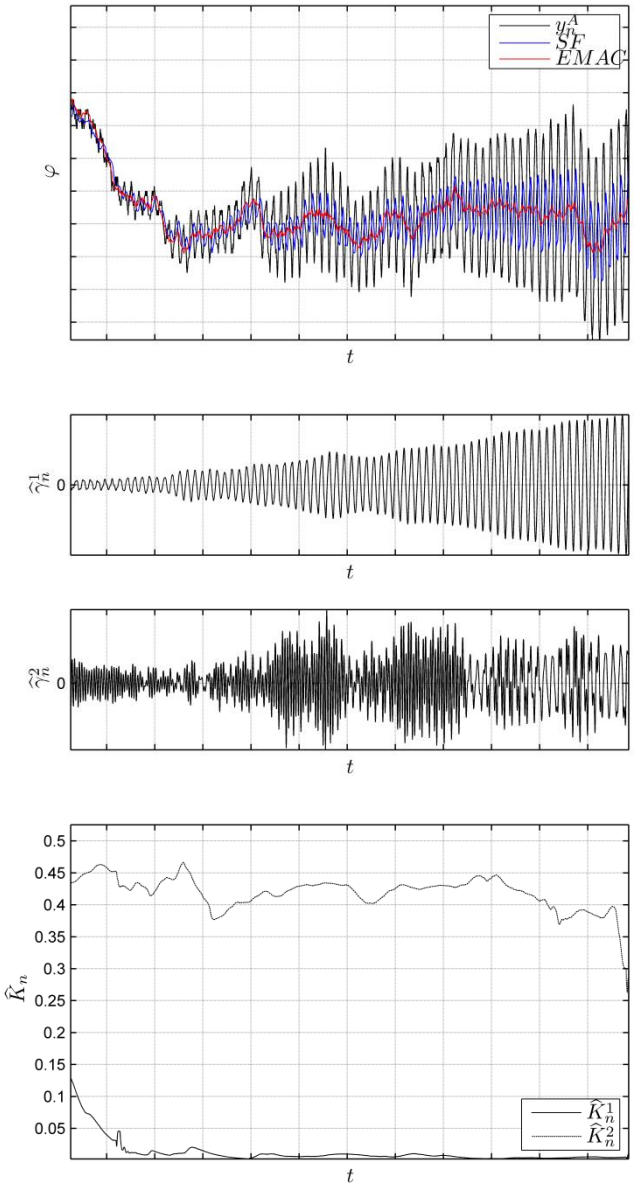

Figure 6: EMAC test bench results using buffet exploration flight testing data. Measured and filtered roll attitude φ generated by the current boom CLAWS filtering method SF in blue, and by the EMAC algorithm in red (top). EMAC estimated $\hat{\gamma}_n^1$ and $\hat{\gamma}_n^2$ elastic mode amplitudes (middle). EMAC estimated perfect cancellation parameters $\widehat{K}_n^1$ and $\widehat{K}_n^2$ (bottom).

6.2 Test Bench Results: Hard Contacts Occurrences During Flight Testing

EMAC algorithm performances in the presence of fast varying exogenous boundary conditions and undetected operational phase transitions will be illustrated by feeding the test bench with flight test data recorded during a hard contact occurrence. In this manoeuvre, the boom operator performs a tracking of the receiver aircraft to finally make the contact in the refuelling receptacle (UARRSI). In this particular test, instants before the transition to coupled condition, the boom nozzle leans on the receiver receptacle slipway, being the flying boom CLAWS still in CL2 mode (free-air mode) before the contact was made. Consequently, there is an undetected boundary condition change during a limited period of time before the system automatically identify the phase transition by means of the receptacle laches pulse when contact is achieved.

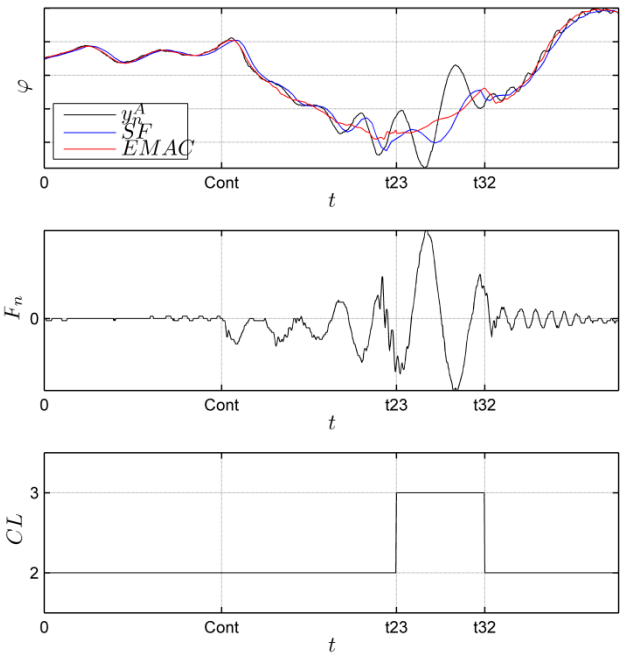

Figure 7: EMAC test bench results using hard contact flight testing data. Measured and filtered roll attitude generated by the current boom CLAWS filtering method SF in blue, and by the EMAC algorithm in red (top). Measured nozzle loads during the test (middle). Flying boom CLAWS internal state values. CL2 denotes free-air phase and CL3 denotes coupled phase (bottom).

Results obtained with the EMAC test bench have been depicted in Figures 7 - 8. As it can be observed, the EMAC algorithm is capable of recognizing the boundary conditions transition maintaining an adequate elastic mode cancellation performance due to the exogenous boundary conditions estimator, even when the flying boom CLAWS internal state is still indicating a free-air condition (CL2). During the instants where an undetected operational phase transition occurs (from t=$Cont$ to t=$t23$) results obtained with [3] show a slight degradation of the simple spatial filter performance.

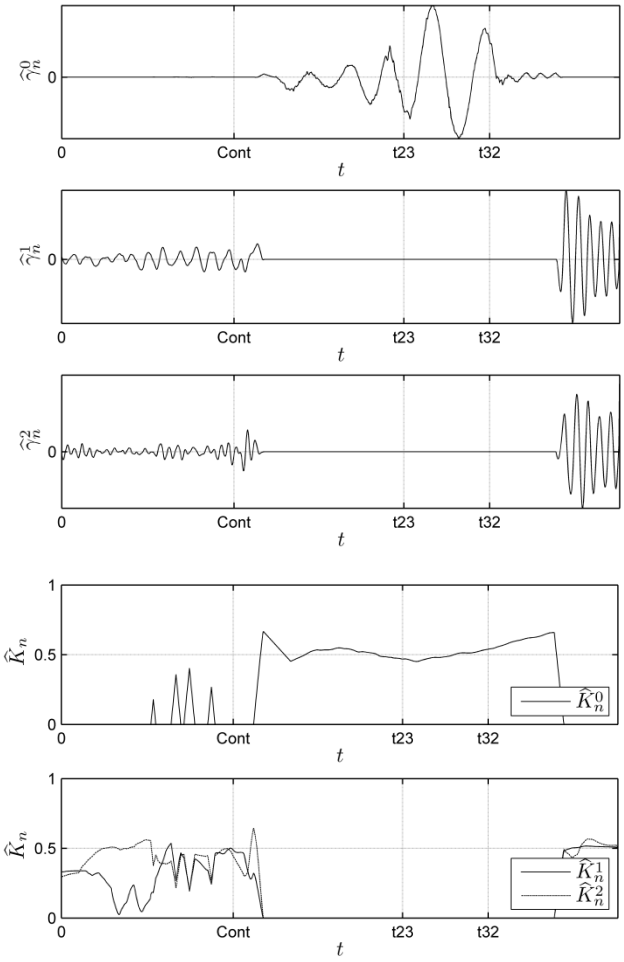

Figure 8: EMAC test bench results using hard contact flight testing data. EMAC estimated elastic mode amplitudes for free-air identified boundary condition $\hat{\gamma}_n^1$ and $\hat{\gamma}_n^2$, and $\hat{\gamma}_n^0$ denoting the estimated elastic mode amplitude for identified coupled boundary condition (top). EMAC estimated perfect cancellation parameters $\hat{K}_n^1$, $\hat{K}_n^2$ (estimated free-air condition) and $\hat{K}_n^0$ (estimated coupled condition) (bottom).

7 Conclusions

The Elastic Modes Adaptive Cancellation algorithm has been developed to overcome the limitations of existing filtering algorithms to isolate the rigid dynamic with zero phase loss and attenuation in a feedback signal of a controlled system. With the use of a very limited number of sensors (only two are necessary), and with a limited previous knowledge of the elastic characteristics of the system (only frequency and elastic mode shape bounds are required), this algorithm has proved to be capable of cancelling all existing elastic modes. Algorithm adaptation is achieved through a set of estimation kernels that identifies in real the elastic modes characteristics of the controlled system. A special observer which estimates the boundary conditions acting on the system reconfigures the bounds applicable to the estimation kernels to make the filtering robust against undetected exogenous boundary conditions transitions.

The EMAC algorithm has been validated offline using recorded data from different flight test campaigns with the A330 MRTT and the A310 MRTT. This algorithm is expected to be implemented in an experimental release of the flying boom flight CLAWS to validate its efficiency and to measure the magnitude of the positive impact on the handling qualities during the refuelling operations.

Although EMAC algorithm has been developed specifically for the A330 MRTT boom control laws, it can be implemented as part of the CLAWS of any flexible system with more than one sensor located along the structure. In addition, EMAC could be used not only to filter the elastic component in the feedback signals, but also to control the elastic dynamics by using a parallel CLAWS with a feedback composed by the elastic modes displacements identifies by the estimation kernels.

References

[1] Roger W. Pratt. *Flight control systems: practical issues in design and implementation*. 1st edition, The Institution of Electrical Engineers, 2000

[2] L.R. Felt, L.J. Huttsell, T.E. Noll, D.E. Cooley. Aeroservoelastic Encounters. *Journal of Aircraft*, Vol 16, pp. 477–483, 1979

[3] C. Avila Aparicio, D. Pelaez Fernandez and M. Barrio Mendez. *Methods and systems for reducing the phenomenon of structural coupling in the control system of an in-flight refuelling boom*. Patent Publication Number US 20090292406 A1, 2009.

[4] Wolfgang Luber. Aeroservoelastic flight control design for a military combat aircraft weapon system. *ICAS*, Brisbane, Australia, 669, 2012

[5] S.A.Halsey, R.M.Goodall, B.D.Caldwell, J.T.Pearson. Filtering Structural Modes In Aircraft: Notch Filters Vs Kalman Filters. *IFAC*. Prague, Czech Republic. 3209, 2005

[6] L. Meirovitch and H. Baruh. The implementation of modal filters for control of structures. *Journal of Guidance*, Control, and Dynamics, Vol. 8, No. 6, pp. 707-716, 1985

[7] R. Rodríguez, J.A. Escobar. Spatial Filter Design for Observation Spillover Suppression. *XXIII Conference and Exposition on Structural Dynamics.* Orlando, Florida. Vol 3, 25A, 1459-1468, 2005

[8] Bor-Sen Chen, Tsang-Yi Yang, Bin-Hong Lin. Adaptive notch filter by direct frequency estimation. *Signal Processing.* Volume 27, Issue 2, pp 161-176

[9] P. A. Regalia and P. A., A complex adaptive notch filter, *IEEE Signal Process. Lett*., vol. 17, no. 11, pp. 937-940, 2010

Copyright Statement